sustainability

MDPI

Article

Advanced Thermal Insulation Plasters Derived from Hazelnut Shell Waste: A Comprehensive Experimental Research

Pinar Mert Cuce [1,2,*], Erdem Cuce [3,4] and Emre Alvur [3]

[1] Department of Architecture, Faculty of Engineering and Architecture, Recep Tayyip Erdogan University, Rize 53100, Turkey
[2] College of Built Environment, Birmingham City University, Birmingham B4 7BD, UK
[3] Department of Mechanical Engineering, Faculty of Engineering and Architecture, Recep Tayyip Erdogan University, Zihni Derin Campus, Rize 53100, Turkey; erdemcuce@gmail.com (E.C.); emre.alvur@erdogan.edu.tr (E.A.)
[4] University Centre for Research and Development, Chandigarh University, Mohali 140413, India
* Correspondence: mertcuce@gmail.com

Abstract

Reducing thermal losses through building envelopes remains a key strategy in the pursuit of low-carbon, energy-efficient buildings. This study presents an innovative and sustainable retrofitting approach involving thermal insulation plaster modified with finely ground hazelnut shells, an abundant agricultural by-product in Türkiye. The modified plaster is applied symmetrically on both sides of standard masonry briquettes in varying proportions (2%, 4%, and 6%), and its thermal performance is experimentally assessed via the laboratory-scale coheating test method. The results reveal a substantial reduction in U-values compared to the uninsulated briquette (5.5 W/m^{2}K): the 2% shell-modified plaster achieves a U-value of 2.40 W/m^{2}K (56.4% improvement), the 4% variant achieves 2.14 W/m^{2}K (61.1%), and the 6% formulation performs best at 2.04 W/m^{2}K (62.9%). In terms of effective thermal conductivity, the modified plasters exhibit values in the range of 0.0408–0.04856 W/mK. Additionally, the 6% composition exhibits enhanced thermal inertia, delaying internal heat loss and offering extended indoor comfort. All samples demonstrate exceptional measurement repeatability, with day-to-day U-value variation below 2%. These findings surpass thermal performance benchmarks reported in previous studies using bamboo or plaster thickness alterations, and position hazelnut shell-modified plaster as a high-potential solution for sustainable building retrofits. The outcomes offer practical implications for low-cost housing, rural construction, and building refurbishment programmes, while also informing policymakers and material standardisation bodies about scalable bio-based alternatives that align with circular economy and decarbonisation goals.

Keywords: building envelope retrofitting; agricultural waste reuse; hazelnut shell; coheating test; sustainable construction; energy-efficient buildings

Academic Editor: Antonio Caggiano

Received: 29 July 2025
Revised: 21 August 2025
Accepted: 8 September 2025
Published: 11 September 2025

Citation: Cuce, P.M.; Cuce, E.; Alvur, E. Advanced Thermal Insulation Plasters Derived from Hazelnut Shell Waste: A Comprehensive Experimental Research. *Sustainability* **2025**, *17*, 8209. https://doi.org/10.3390/su17188209

1. Introduction

Buildings are among the largest consumers of energy worldwide, contributing significantly to greenhouse gas emissions. In many countries, the building sector accounts for a substantial share of total energy use. For example, it accounts for around 40% of energy consumption in the UK [1]; around 31% of final energy consumption and 30% of greenhouse gas emissions in Türkiye [2]; nearly 26% of overall energy consumption in India, with projections suggesting that this could rise to 40% by 2040 if current trends continue [3];

and approximately 40% in China as well [4]. This outsized energy demand translates into considerable carbon emissions; globally, buildings (operations) are responsible for roughly 28–39% of energy-related CO_2 emissions [5,6]. Such figures have raised alarms in the context of climate change and sustainability. Under the Paris Agreement, nations have set ambitious targets for the coming decades. For instance, the UK aims for a 78% emissions reduction by 2037 (en route to net-zero by 2050) [7], whilst China's energy strategy intends to cap total energy use by 2030 and raise the share of non-fossil energy to 20% [8]. India and Turkey have likewise committed to substantial efficiency improvements and emissions cuts by 2030 in their nationally determined contributions. Achieving these goals will require tackling the building sector's energy use head-on. The United Nations' Sustainable Development Goals (SDGs) reinforce this imperative: SDG 7 (Affordable and Clean Energy) calls for doubling the global rate of energy efficiency improvement by 2030 and expanding access to sustainable energy; SDG 13 (Climate Action) urges urgent measures to combat climate change; and SDG 11 (Sustainable Cities and Communities) emphasises the need to make buildings more inclusive, safe, resilient, and sustainable, particularly by improving energy performance and reducing their environmental impact [9]. In this context, reducing energy consumption in buildings, particularly for heating and cooling, has become a critical priority on the path to a sustainable future.

One of the most effective strategies to cut building energy demand is to improve the thermal performance of the building envelope. The building envelope (exterior walls, roofs, windows, etc.) is the interface through which most heat exchange occurs between indoors and outdoors. If poorly insulated, the building envelope as a whole (including walls, roofs, and openings) becomes a major source of energy loss. Studies show that external walls alone can account for 40% of a building's heat loss (with roofs and floors adding ~15–25%, and windows/doors another ~25–47%) [10]. In other words, a large portion of the energy used to heat or cool a building literally leaks out through the facades. This not only wastes energy but also undermines indoor comfort. Conversely, improving envelope insulation has a dramatic impact on efficiency. By some estimates, optimising the thermal properties of walls, windows, and roofs can reduce a building's energy consumption by 20–50% [11]. Indeed, controlling heat transfer through the exterior (for example, adding insulation to walls) can directly cut the heating/cooling load, thereby lowering fuel or electricity use. This reduction in demand creates a virtuous cycle: buildings require less energy from the grid or boilers, thus facilitating a faster transition to renewable energy sources by relieving some of the pressure on the energy supply. In essence, insulating building facades is a bridge strategy that buys time and carbon savings while cleaner energy infrastructures are being developed. It also offers immediate benefits in terms of lower energy bills and improved thermal comfort for occupants. Given that buildings last for decades, upgrades made now (such as high-performance insulation) will continue to yield energy and emissions reductions through 2030, 2040, and beyond. For these reasons, envelope insulation is widely recognised as a key measure for sustainable buildings, reflected in building codes and retrofitting programs worldwide. This decade has been deemed "crucial for implementing the measures required" to make all new buildings and a sizable portion of existing ones "zero-carbon-ready" by 2030 [12]. To effectively realise these goals, recent research has increasingly focused on innovative facade insulation strategies. In particular, three areas have drawn considerable attention: thermally efficient plaster systems; insulation materials derived from sustainable or waste-based sources; and ultra-low-conductivity materials, such as aerogels. Thermal insulation plasters, especially when enhanced with eco-friendly additives, offer an adaptable and cost-effective route for both new constructions and retrofits. Meanwhile, bio-based or recycled insulation materials align with circular economy principles, helping reduce the embod-

ied carbon of buildings. Lastly, aerogels represent a cutting-edge frontier for ultra-thin, high-performance facade systems thanks to their exceptional thermal resistance. The following literature review explores recent advances and findings in these domains, laying the groundwork for material-driven strategies to reduce building energy consumption while enhancing sustainability.

Fattahi et al. [13] explored the dual function of corn husk fibres as both thermal insulators and sound absorbers in building applications. Their study reports effective thermal conductivity values between 0.038 and 0.042 W/mK, largely unaffected by moisture content, and notes a strong sound absorption capacity (SAC > 0.5 at >1 kHz), which improves with greater sample thickness and density. These findings underline corn husk fibres as promising candidates for multifunctional bio-based insulation systems that enhance both energy efficiency and acoustic comfort. Yang et al. [14] conducted an experimental assessment of straw bale walls, evaluating how structural details, such as bale joints, rebar arrangements, and finishing layers, influence thermal performance. Their results demonstrate that avoiding straw bale joints and applying lime plaster significantly reduce U-values, with the lowest recorded at 0.48 W/m^{2}K under optimised pre-compression and surface sealing. Their study reinforces the critical role of construction detailing in realising the full insulation potential of bio-based materials. Shea et al. [15] presented extensive laboratory and modelling work on straw bale insulation, establishing a representative thermal conductivity of 0.064 W/mK and a corresponding U-value of 0.178 W/m^{2}K for prefabricated panels. Their study highlights the influence of straw orientation, density, temperature, and relative humidity on thermal behaviour, offering crucial benchmarks for natural fibre insulation design. Seifhashemi et al. [16] evaluated the energy-saving potential of internal wall insulation in solid wall dwellings, using a validated building simulation model based on the Salford Energy House. Their findings show that internal wall insulation can reduce heating demand by 19–46.2% depending on baseline U-values (ranging from 0.64 to 2.48 W/m^{2}K), with annual CO_2 savings reaching 1248 kg and notable improvements in thermal comfort. Platt et al. [17] investigated the thermal and hygric performance of three bio- and waste-based insulation prototypes. Among them, the straw-based panel demonstrated the most stable U-value (average 0.29 W/m^{2}K) across varying environmental conditions, whereas maize pith's performance was highly sensitive to humidity. Dams et al. [18] evaluated five full-scale bio-based wall systems using sheep's wool, wood fibre, mycelium, and cellulose insulation, reporting U-values between 0.13 and 0.22 W/m^{2}K. Their results confirm that such walls can meet or exceed regulatory benchmarks, offering both thermal and hygric stability under real and simulated environmental conditions. Elkhayat et al. [19] complemented this growing literature by simulating five conventional insulation types in Egyptian residential flats using DesignBuilder v6.5 software. Their study highlights extruded polystyrene (XPS) as the optimal solution, offering the highest energy savings (9.72%) and extending thermal comfort hours by 33% annually. Cuce et al. [20] tried to investigate how briquettes, which are widely used in Anatolia, can be made thermally resistant. To do this, they used an improved insulation plaster, which has no carcinogenic material inside, and this plaster was coated on the briquettes with altering thicknesses. Their result demonstrated that their plaster effectively resisted the briquettes; for example, if the plaster was covered with a 20 mm thickness on both sides, the U-value decreased from 5.5 W/m^{2}K to 2.86 W/m^{2}K. The same strategy goes through with the bamboo investigated by Cuce et al. [21]. In this study, they made a briquette sample with different percentages of bamboo. To be able to test for the results, their strategy was to perform the coheating test. Nevertheless, their overall results indicated that the one with the highest percentage of bamboo briquette (6%) showed the best resistance against the heat transfer. Kamble et al. [22] provided experimental validation

of porous brick walls integrated with green insulation, demonstrating a 57.15% reduction in heat load under optimal porosity (30%) and patterning. Bendaikha et al. [23] supported this growing body of evidence by demonstrating that insulation blocks fabricated from raw and milled pine needles offer highly competitive thermal conductivity values (0.0228–0.0238 W/mK) with remarkably low densities (28.57–32.72 kg/m^3), rivalling commercial sandwich panels. Among the tested variants, dried raw pine needles oriented perpendicular to heat flow showed superior performance regarding temperature gradient and thermal resistance. Messahel et al. [24] investigated low-cost insulation panels made from cement and horizontally placed plastic bottles filled with reused materials. Their results indicated that plastic bag-filled bottles mitigate U-values by 60% compared to sand-filled variants, revealing the viability of lightweight plastic waste in improving the thermal efficiency of low-income housing. Rashid et al. [25] extended this exploration into clay-based masonry units by incorporating natural and synthetic fibres such as coir, bamboo, jute, and polyester into traditional bricks. Their results indicated that fibre inclusion reduces bulk density and thermal conductivity by up to 18%, with coconut coir exhibiting the highest insulation improvement. Charai et al. [26] explored the use of Moroccan non-industrial hemp fibres as partial bio-aggregate replacements in plasterboards for thermal insulation enhancement. Their results show that adding up to 6% hemp fibres significantly decreases plaster density and thermal conductivity by 24.5% and 31.3%, respectively, while also improving passive cooling performance in semi-arid climates. Nasreddine et al. [27] explored the reuse of human hair fibres in cement mortars, demonstrating a 37% reduction in thermal conductivity (down to ~0.037 W/mK) with 8 wt% human hair fibre addition, while maintaining adequate compressive strength. Ali et al. [28] investigated the thermal performance of sustainable and waste materials. They first dried the waste materials and then made them into a paste with glue. Those samples were then put into the thermal conductivity meter to examine the thermal performance. Their results show that pineapple leaf fibre has the highest thermal resistance. Ba et al. [29] investigated the thermal performance of bio-based composites by incorporating *Typha australis* as a natural insulation material. They reported that the addition of it significantly reduced thermal conductivity, from 0.8 to 0.1 W/mK in cementitious matrices and from 12.06 to 0.15 W/mK in clay–cement blends, resulting in energy savings of up to 22% in building applications. Although the mechanical strength decreased, the thermal benefits highlighted the material's strong potential for energy-efficient construction. Łapka et al. [30] examined bio-based composites made from hemp shives and a magnesium binder, enhanced with microencapsulated phase change material (PCM), to improve thermal mass and insulation performance. They showed that increasing PCM content generally decreases thermal conductivity, reaching as low as 0.105 W/mK in dry conditions, while moisture and temperature variations significantly influence performance. Blanco et al. [31] assessed the thermal performance of masonry walls incorporating by-products such as lime sludge and sawdust, using both numerical modelling and experimental validation. They found that walls made with sawdust blocks reduced U-values by up to 10.5%, and when combined with recycled cellulose insulation, improvements reached up to 33.3% compared to conventional concrete blocks. Briga-Sá et al. [32] investigated the thermal performance of cement-based lightweight blocks incorporating 6.25–8.75% textile waste comprising 70% wool, 25% viscose, and 5% elastane. Their results showed that increasing textile waste content improves thermal resistance, corresponding to U-values decreasing from approximately 2.94 W/m^{2}K to 1.49 W/m^{2}K, making the material more effective for insulation purposes. El-Lawindy et al. [33] also focused on clay bricks, demonstrating that incorporating up to 20% sugarcane-derived cellulose fibres significantly improves insulation capacity. Their simulations showed a 44.7% reduction in thermal conductivity, a 39.1% drop in heating electricity use, and a 63.3% decline in

CO_2 emissions. Ahmed et al. [34] examined the use of fired clay bricks incorporating 15% pomegranate peel waste as a strategy for improving thermal insulation and sustainability in construction. The optimised bricks demonstrate a significantly lower thermal conductivity (0.25 W/mK), translating to a 33.13% reduction in cooling energy demand and a 24.53% decrease in CO_2 emissions compared to conventional bricks. Their cost-effectiveness, with a payback period as short as 1.88 years, highlights their strong potential for application in hot and arid climates. Ahmed et al. [35] proposed the integration of industrial wastewater sludge treated via mycelium processes as a clay substitute in fired bricks. Bricks with 20% industrial wastewater sludge fired at 900 °C exhibit a 0.198 W/mK thermal conductivity and lead to up to 39% energy savings in hot climates. In parallel, recent advances also illustrate how non-agricultural wastes can be valorised into thermally functional building materials. For example, synergistic preparation of ceramic foams from wolframite tailings and high-borosilicate waste glass demonstrates the potential of industrial by-products to yield lightweight, porous structures with favourable thermal and mechanical properties [36]. Similarly, cascade pyrolysis of acid hydrolysis lignin enables the cooperative production of monophenolic chemicals and high-surface-area carbon adsorbents, highlighting novel pathways for lignin utilisation in construction-related applications [37]. Ozocak and Sisman [38] explored the feasibility of producing insulation boards using hazelnut shells, an agricultural waste material abundantly available in certain regions. Two types of boards were fabricated using 80% and 90% shell content, with epoxy as the binder. The boards exhibited thermal conductivity values between 0.136 and 0.148 W/mK, along with notable acoustic insulation performance. Cuce et al. [39] assessed the effectiveness of 20 mm thick aerogel blanket retrofitting in a traditional 1930s UK house using a full coheating test. They found that the heat loss coefficient of the retrofitted bedroom dropped from 17.15 W/K to 6.29 W/K, equating to a 63% reduction in heat loss. However, subsequent investigations revealed that internal retrofitting may inadvertently intensify heat losses through uninsulated building components, particularly separating walls, due to pronounced thermal bridging effects, where post-retrofit heat loss rises from 0.66 to 5.86 W/m^2 [40]. This research underlines the importance of comprehensive envelope analysis, including thermal bridge detection and mitigation, before implementing internal thermal super insulation strategies. Arregi et al. [41] investigated a bio-based, multilayered wall system employing biocomposite framing profiles, achieving U-values between 0.27 and 0.30 W/m^2K when installed correctly. Additionally, aerogel and vacuum insulation panels (VIPs) are identified as promising solutions due to their ultra-low thermal conductivity; yet issues such as cost, durability, junction detailing, and indoor space reduction constrain their widespread adoption [42]. While internal thermal super insulation benefits from minimal thickness and aesthetic integration, external retrofitting offers better continuity and protection from environmental degradation. The abovementioned studies collectively conclude that the combined use of aerogel with conventional materials, along with careful treatment of thermal bridges, is key to achieving high-efficiency, low-carbon retrofitting in line with future net-zero energy goals.

In parallel with opaque facade improvements, enhancing the thermal performance of fenestration systems is equally essential due to their significant role in total building heat loss. Several recent studies introduce and evaluate next-generation window technologies that outperform conventional double glazing in terms of U-value, energy savings, and retrofit suitability. Cuce et al. [43] developed a thermally resistive photovoltaic glazing (TRPVG-Ar16) which integrates argon-filled layers behind an amorphous silicon PV module. Numerical and experimental results show that a 20 mm argon gap provides the optimum thermal performance, yielding U-values of 1.192 W/m^2K (CFD) and 1.135 W/m^2K (coheating test). Beyond this thickness, natural convection becomes dom-

inant factor, increasing the heat transfer rate. Importantly, thermal bridging caused by metallic spacers is effectively mitigated through PVC-U edge seals, confirming the suitability of TRPVG-Ar16 for low/zero carbon retrofits. In cold-climate applications, Pourghorban and Asoodeh [44] showed that advanced glazing units in Trombe wall systems reduced heating periods by nearly 49% and extended comfort conditions by 23.9%, underscoring the impact of glazing on passive envelope technologies. Complementary findings in Mediterranean conditions by Simões et al. [45] demonstrated that Trombe walls, combined with shading and night ventilation, achieved over 20% heating demand reduction and 35% cooling demand savings in southern locations. Parallel developments are evident in PV-integrated facades. Cuce [46] introduced the vacuum tube window concept, composed of evacuated cylindrical glass elements surrounded by argon, achieving U-values below 0.40 W/m^2K and validated experimentally. Liu et al. [47] expanded on this direction with semi-experimental investigations of PV double-skin facades (PV-DSFs), concluding that 40% semi-transparent PV glass with double-glass backing yields 22.7% and 16.8% energy savings in summer and winter, respectively. Peng et al. [48] further assessed ventilated PV-DSFs, showing that active ventilation reduces SHGC to 0.10 and increases electricity yield by 1.9–3% compared with non-ventilated designs, confirming the necessity of adaptive operating strategies in subtropical climates. Advanced thermochromic solutions also represent a key research frontier. Essakali et al. [49] reported that combining thermochromic and electrochromic coatings in double glazing can cut energy consumption by 26% while improving visual comfort. Hong et al. [50] demonstrated, via multi-objective optimisation, that thermochromic glazing reduces energy demand to 44.4 kWh/m^2 whilst maintaining over 70% daylight autonomy. Butt et al. [51] complemented this by modelling thermochromic coatings on opaque building envelopes across climates, identifying 2–13% annual energy savings when switching temperatures are tuned to building type and location. Novel insulation concepts have also been explored. Zakaria et al. [52] evaluated smart double-glazed windows incorporating aerogel and argon, with respective heat transfer reductions of 21% and 59%. Abdelrady et al. [53] confirmed that nanogel glazing achieves annual energy savings of up to 26% in hot desert climates. Li and Wu [54] provided a broader review of complex glazing systems, identifying vacuum and aerogel-based units with U-values below 1 W/m^2K as optimal in heating-dominated regions, while electrochromic and semi-transparent PV glazing offer advantages in cooling-dominated contexts. The solar pond window by Cuce and Cuce [55] achieved a U-value of 0.40 W/m^2K for EUR 120/m^2, exemplifying material economy alongside efficiency. Hybrid PV–vacuum technologies further push performance boundaries. Tan et al. [56] presented CdTe-based vacuum–PV glazing validated experimentally at 0.92 W/m^2K, achieving 60% reductions in heat losses and gains with annual PV outputs of 34–48 kWh/m^2. Radwan et al. [57] compared multiple hybrid systems and showed that PV–vacuum glazing achieves the lowest U-values (1.2 W/m^2K) and eliminates condensation risks, outperforming other smart glazing variants. Ghosh et al. [58] experimentally measured semi-transparent PV–vacuum glazing, reporting a U-value of 0.8 W/m^2K and a solar factor of 0.42–66% and 46% lower than PV double glazing, confirming its suitability for cold climate retrofits. At the system scale, Lami et al. [59] proposed an active double-glazing unit with air injection, reducing window thermal losses by 52% and heating energy by 19%. Naqash [60] provided design recommendations that favour argon-filled triple glazing with low-e coatings in hot and dry regions. Awale and Uprety [61] demonstrated that optimising the window-to-wall ratio cuts energy use by 9–15%, while Vijayan et al. [62] emphasised, through case studies, that advanced glazing, such as aerogel, can reduce window heat gains by up to 57% relative to single glazing. At the national scale, Sia and Ariff [63] highlighted that advanced

glazing and envelope technologies underpin Malaysia's Green Building Index Platinum achievements, cutting total building energy use by 65% and energy intensity by 66%.

Despite the expanding body of literature on bio-based and waste-derived thermal insulation materials, limited attention is given to the incorporation of agricultural by-products into thermally insulating plasters specifically tailored for application on masonry briquettes. Moreover, few studies combine both front and rear surface treatment using natural waste additives within the plaster matrix to assess bilateral thermal resistance under realistic boundary conditions. Addressing this gap, the present study introduces an innovative facade enhancement strategy by embedding finely granulated hazelnut shells, an abundant yet underutilised agricultural waste, in varying concentrations (2%, 4%, and 6%) into a 10 mm thick thermal insulation plaster applied symmetrically on both faces of traditional briquette units. The thermal performance of these modified briquette systems is then rigorously assessed using the coheating test method to determine both thermal conductivity and overall heat transfer coefficients (k- and U-values). This research not only explores a novel utilisation route for hazelnut shell waste but also offers a scalable and sustainable envelope retrofitting solution suitable for low-income housing or rural construction contexts. What differentiates hazelnut shells from previously tested bio-based additives like pine needles, coconut fibres, or textile waste is their unique chemical and morphological profile: a notably high lignin content (40–51%), rigid shell fragments with inherent porosity, and low moisture permeability. This combination imparts both structural stability and superior thermal resistance, providing a fundamentally different insulation mechanism and enabling U-value reductions beyond those reported for earlier bio-based composites. The outcomes are expected to yield insights into the optimal mix design for enhanced thermal resistance, thereby contributing to the development of cost-effective, eco-friendly facade systems aligned with circular economy and low-carbon building targets.

2. Material and Method

2.1. Hazelnut Shells

Hazelnut shells constitute a readily available lignocellulosic by-product that is generated in large quantities throughout Türkiye, the world's leading hazelnut producer. As of 2022, national production reaches approximately 765,000 tonnes, with the majority concentrated in the Black Sea Region [64]. The de-shelling process produces a substantial amount of shell residue, accounting for approximately 50–55% of the in-shell nut mass [65]. Traditionally, these shells are utilised as low-efficiency solid fuel or agricultural mulch; however, their combustion contributes to elevated particulate matter emissions and environmental degradation. Such conventional uses fail to fully exploit the material's potential. Conversely, converting hazelnut shells into insulation panels or lightweight plasters aligns with circular economy principles, mitigates environmental impact, and valorises an otherwise discarded agricultural residue. Structurally, hazelnut shells are rich in lignocellulosic content, comprising primarily lignin (40–51%), cellulose (17–27%), and hemicellulose (13–32%) [65]. This chemical composition imparts rigidity, thermal resistance, and low moisture permeability, desirable characteristics for construction material applications. Their fibrous morphology and relatively low density support their incorporation into lightweight composites, whilst their inherent porosity offers potential advantages in both thermal insulation and acoustic attenuation. In terms of thermal behaviour, hazelnut shells demonstrate relatively low intrinsic thermal conductivity, typically ranging between 0.10 and 0.15 W/mK, depending on processing conditions. These properties render them suitable for integration into building envelope components where passive thermal regulation is required. In the present study, hazelnut shells of the "Giresun Tombul" variety are sourced directly from local agricultural producers in Giresun, Türkiye. Following initial

cleaning and drying, the shells are mechanically crushed and sieved to achieve a bimodal particle distribution: approximately 70% fine particles (<3 mm) and 30% coarse fragments (3–6 mm). This mixture is subsequently incorporated into a cement-based thermal insulation plaster at varying volume fractions of 2%, 4%, and 6%. The modified plaster is applied in 10 mm thick layers to both the front and rear faces of specially prepared lightweight masonry units. To ensure uniform dispersion and optimal binding, the plaster mixture is homogenised using a mechanical mixer, with a constant water-to-binder ratio maintained across all samples. The hazelnut shell particles function as lightweight fillers, contributing to both reduced thermal conductivity and decreased bulk density of the final material. All test specimens undergo curing under standard laboratory conditions for 28 days prior to thermal performance evaluation.

2.2. Detailed Preparation Process of Briquettes Coated with Hazelnut Shell-Modified Insulation Plaster

In this experimental study, hazelnut shells sourced from Giresun, a province in the Black Sea Region of Türkiye, where hazelnut production is a dominant agricultural activity, are utilised as a bio-based additive in insulation plaster. The shells are supplied in a pre-broken form, having been mechanically separated from the kernel. They typically arrive split into two halves and in irregular fragments, making them suitable for further mechanical processing. The shells are initially subjected to a coarse crushing process to reduce them to manageable sizes. To ensure the preservation of their fibrous structure and to eliminate residual moisture, the crushed shells undergo a solar drying process. This drying is conducted in Rize province using a custom-designed solar drying system powered entirely by renewable solar energy. The system is designed to reach internal air temperatures ranging between 45 °C and 60 °C, which is sufficient to remove internal moisture content without degrading the lignocellulosic composition of the shells. The solar drying process not only helps in retaining the natural fibre integrity of the hazelnut shells but also enhances their compatibility with cementitious materials by reducing water activity. This prevents microbial degradation and ensures long-term stability when incorporated into plaster. Once drying is complete, the shells are subjected to a secondary fine-grinding operation to obtain smaller, more uniform particles that are more suitable for even distribution within the plaster matrix. These particles are then blended with a microfibre-reinforced base insulation plaster in varying replacement ratios by weight, 2%, 4%, and 6% respectively, to obtain new formulations of modified plaster. Water is gradually added to each mixture, and the mixtures are mechanically mixed for approximately 10 min until a uniform and homogenous mortar consistency is achieved. Care is taken to monitor the workability and avoid segregation of materials during the mixing process. Following the preparation, the newly developed plasters are applied to both the front and rear surfaces of standard concrete briquettes, which are widely used in Anatolian construction stock. Each coating layer is applied with a uniform 10 mm thickness, using moulds to ensure dimensional accuracy and surface consistency. After application, the specimens are left to cure under ambient conditions for 28 days, allowing the hydration reactions and moisture evaporation processes to complete. Upon curing, these samples are prepared for thermal performance characterisation using the coheating test method, which allows for the precise measurement of the heat loss and insulation efficiency across the composite briquette surfaces. The overall preparation process is illustrated in Figure 1, which visually summarises the key steps already detailed in the text, from raw material acquisition to sample readiness for thermal evaluation.

Figure 1. Flowchart of the preparation process for hazelnut shell-modified insulation plaster applied on briquette surfaces.

2.3. Coheating Test Method

The coheating test is a semi-stationary and controlled experimental technique widely employed to evaluate the U-value of building envelopes by establishing the relationship between the net heat input and the temperature differential between internal and external environments [66]. Even though it is initially designed for full-scale, in situ assessments of entire buildings, its application has increasingly expanded to laboratory-scale settings [67], particularly for evaluating the thermal performance of individual construction components or novel insulation materials under reproducible and tightly regulated conditions. In this study, a laboratory-based coheating test is implemented to examine the thermal performance of an innovative bio-based plaster incorporating hazelnut shell particles. The test protocol is designed under the core principles of the classical coheating method, with specific adaptations tailored to the scale and nature of the experimental configuration. The setup consisted of a cubic test chamber (1 m^3 in volume), constructed using 40 mm thick XPS insulation panels to ensure adiabatic boundary conditions on all faces except the test aperture. This hot box is positioned within a larger environmental chamber capable of simulating external climate conditions, with ambient temperatures precisely modulated through an integrated HVAC system to maintain stable "outdoor" settings. A simplified schematic of the test configuration is presented in Figure 2, highlighting the interaction between internal heating, data acquisition elements, and external temperature control mechanisms.

A 500 W fan-driven electric heater, governed by a proportional–integral–derivative (PID) thermostat, is employed to maintain a constant interior air temperature of 25 $\pm$ 0.5 °C. The heating system is activated once the temperature difference between internal and external air exceeds 10 °C, a prerequisite for meaningful heat flux analysis. A briquette coated on both faces with the hazelnut shell-enhanced plaster serves as the test specimen and is installed into a dedicated opening on one face of the box to enable unidirectional heat transfer through the path. The configuration is deliberately designed to eliminate lateral conduction and achieve one-dimensional heat flow, ensuring the validity of calculated thermal transmittance values. Thermal data acquisition is carried out using a data Taker-brand multi-channel data logger, to which all sensors are connected. T-type thermocouples are affixed at the interior and exterior surfaces of the test specimen to monitor surface temperatures, whilst a calibrated heat flux sensor is mounted centrally on the interior face to measure real-time conductive heat flow through the plastered masonry. The heat flux sensor initially records readings in millivolts (mV), which are subsequently

converted into heat flux values in W/m^2 by dividing the raw data by the sensor's specific sensitivity coefficient (expressed in $V/(W/m^2)$), as provided by the manufacturer's calibration data sheet. This conversion enables accurate quantification of the surface heat transfer rate. Following this, the dynamic U-value of the plastered sample is computed at each timestep using the heat flux divided by the corresponding surface temperature differences (ΔT) across the specimen, resulting in instantaneous U-values in W/m^2K. These values are then averaged over the effective test period to yield a representative U-value for the composite insulation system. Each specimen is tested twice under identical boundary conditions to ensure consistency and repeatability. Each individual test lasts approximately 12 h, resulting in 24 h of active data acquisition per sample configuration. These tests are typically conducted over the course of two consecutive days. A portion of each test duration is dedicated to the thermal stabilisation phase, during which the system approaches quasi-steady-state conditions; this initial period is excluded from the U-value averaging process to enhance data accuracy. Throughout the measurement process, thermal data are logged at 5 s intervals, allowing for high-resolution temporal analysis of the thermal responses. Before initiating data acquisition, the entire hot box assembly is meticulously sealed to minimise air leakage and ensure stable boundary conditions. Additionally, an infrared thermographic scan is performed beforehand to identify and eliminate thermal bridges or unintended heat loss paths. This preliminary thermography serves as both a qualitative validation of the test setup and a safeguard against potential inaccuracies caused by infiltration or constructional defects. Figure 3 presents the schematic of the hot box system used in the experiment. It also includes thermographic images confirming negligible thermal leakage.

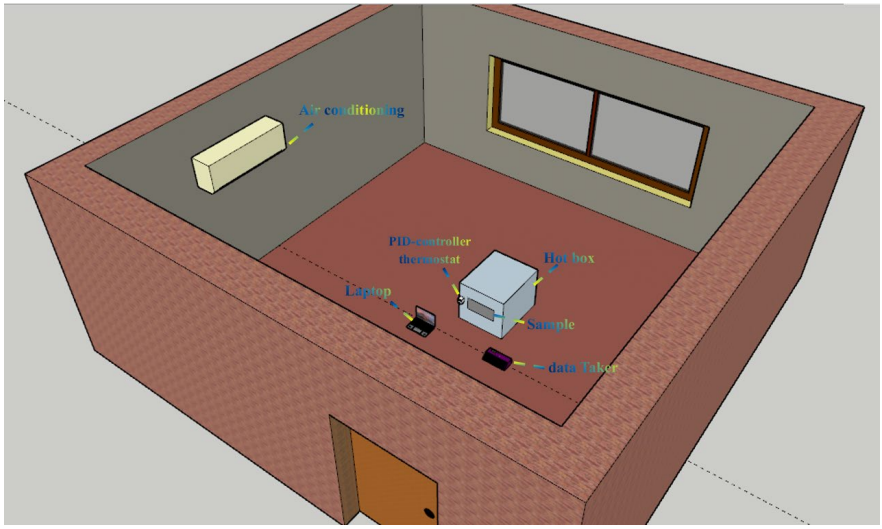

Figure 2. Schematic view of the coheating test setup used for thermal performance evaluation under controlled laboratory conditions.

The laboratory coheating test provided several advantages over conventional field-based applications, most notably the ability to isolate material-specific thermal behaviour without interference from occupant behaviour, solar gains, or uncontrolled ventilation. Additionally, the tightly regulated boundary conditions permitted accurate thermal comparisons across samples under identical test environments. The inclusion of infrared thermography also enhanced the experimental framework by enabling visual interpretation of surface temperature gradients and the detection of potential thermal inconsistencies on the specimen surface. The methodology allowed for both steady-state and transient analysis of the insulation material, supporting a comprehensive evaluation of its thermal

performance. The dynamic resolution of the data enabled detailed thermal characterisation, such as response time to heating cycles, thermal lag, and temperature uniformity across the plastered surface. As a result, this adaptation of the coheating method offers a robust, repeatable, and scientifically rigorous procedure for benchmarking novel, bio-based insulation materials against established thermal performance criteria.

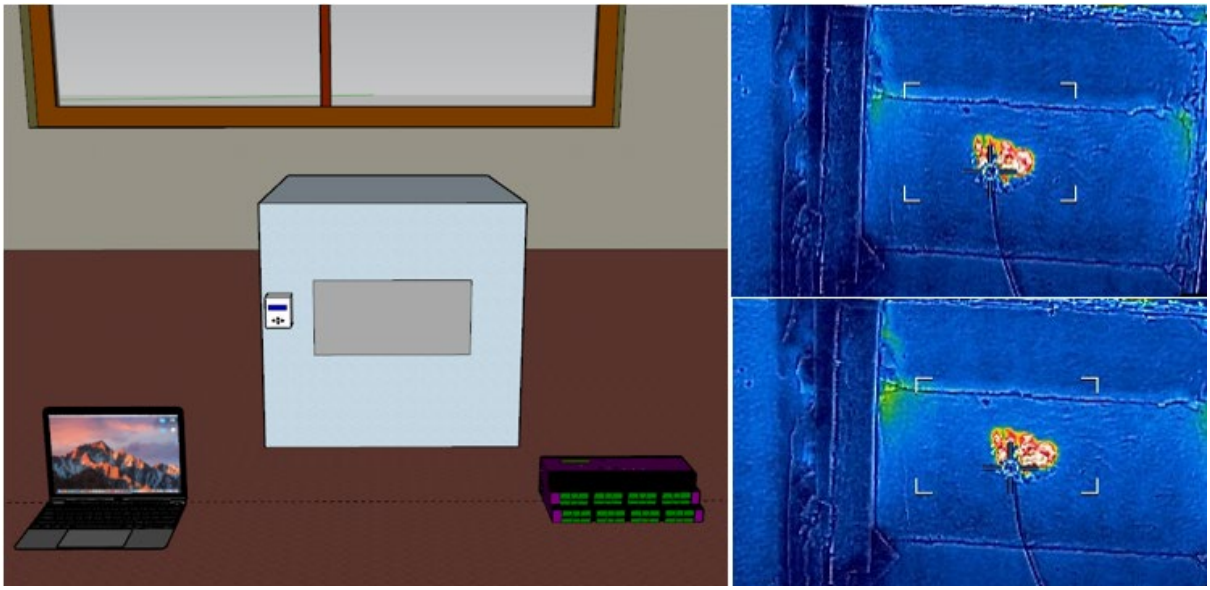

Figure 3. Experimental hot box setup with thermographic validation of minimal thermal leakage.

2.4. Uncertainty Propagation

The combined uncertainty in the evaluation of thermal conductance is assessed through the uncertainty propagation method, which takes into account the partial derivatives of the target variable with respect to the influencing parameters [68]. This standard approach is mathematically described in Equation (1):

$$U_C^2 = \left(\frac{\partial C}{\partial Q} \times U_Q\right)^2 + \left(\frac{\partial C}{\partial \vartheta} \times U_\vartheta\right)^2 \tag{1}$$

In this expression, C is the thermal conductance (W/K), whilst Q represents the rate of heat transfer (W). Additionally, $\Delta\vartheta$ is the temperature difference between indoor and outdoor air (°C), while U_Q and U_ϑ refer to the standard uncertainties associated with heat flux and temperature difference, respectively.

The conductance is derived from the following:

$$C = \frac{Q}{\Delta\vartheta} = \frac{198}{10} = 19.8\,\mathrm{W/K} \tag{2}$$

The relevant sensitivity coefficients are as follows:

$$\frac{\partial C}{\partial Q} = \frac{1}{\Delta\vartheta} = \frac{1}{10} = 0.1 \tag{3}$$

$$\frac{\partial C}{\partial Q} = -\frac{Q}{\Delta\vartheta^2} = -\frac{198}{100} = -1.98 \tag{4}$$

Given the instrumentation used, heat flux sensor uncertainty is ±0.02 W, and thermocouple uncertainty is ±0.15 °C. Nevertheless, the propagated uncertainty in thermal conductance becomes as follows:

$$U_C = \sqrt{(0.1 \times 0.02)^2 + ((-1.98) \times 0.15)^2} = \sqrt{0.002^2 + 0.297^2} \approx 0.3 \quad (5)$$

The relative uncertainty is then calculated as follows:

$$\frac{U_C}{C} \times 100 = \frac{0.3}{19.8} \times 100 \approx 1.5\% \quad (6)$$

Accordingly, the total uncertainty in the thermal conductance evaluation is approximately 1.50%, confirming the reliability and precision of the measurements under the current experimental setup. This value is well within the acceptable threshold for building energy performance assessments.

3. Results and Discussion

Before presenting the thermal performance outcomes, it is important to provide contextual information regarding the experimental procedure. For each plaster formulation, the coheating test is repeated twice under identical laboratory conditions to ensure data consistency, reproducibility, and validation of the observed trends. This dual-testing strategy serves a dual purpose: firstly, it allows for the identification of potential experimental variability or anomalies between runs; and secondly, it strengthens the robustness of the results by demonstrating repeatability. In the present case, the thermal performance of the insulation plastered briquette samples obtained from 2%, 4%, and 6% hazelnut shells is assessed over two consecutive days, with each test lasting approximately 12 h and following a thermal stabilisation period. The results obtained from surface temperatures (both internal and external) and heat flux values form the basis for determining the dynamic U-value and k-value of the tested composite system. The reported U-values are computed from the real-time ratio of heat flux to the temperature difference across the test specimen. The process ensures one-dimensional heat transfer and eliminates lateral losses, thereby enhancing the reliability of the results. The inclusion of repeated trials further supports the credibility of the findings and serves as a practical validation step within the laboratory-scale coheating test methodology.

For a 10 mm thick plaster layer with 2% by weight finely ground hazelnut shell applied to the briquette surface, the first day of testing reveals an internal air temperature between 25.11 °C and 27.29 °C, with an average of 25.74 °C. The external temperature ranges from 18.50 °C to 19.30 °C, averaging 18.88 °C. The heat flux values vary between 5.97 W/m^2 and 115.84 W/m^2, with a mean of 16.89 W/m^2, leading to U-values from 0.91 W/m^{2}K to 15.37 W/m^{2}K and a daily average of 2.40 W/m^{2}K. Considering the applied plaster thickness of 10 mm on both sides (20 mm in total), this U-value corresponds to an effective thermal conductivity of approximately 0.048 W/mK for the composite plaster layer. Figure 4 presents the full set of measurements obtained on the first day, including internal and external air temperatures and heat flux values. Both instantaneous data and daily averages are included for clarity. On the second day, the average internal and external temperatures are 25.597 °C and 18.49 °C, respectively. Heat flux values range from 5.565 W/m^2 to 109.972 W/m^2, averaging 17.54 W/m^2, whilst the U-value spans from 0.824 W/m^{2}K to 13.196 W/m^{2}K, with a daily mean of 2.428 W/m^{2}K. The day-to-day variation in mean U-value is 1.17%, indicating a stable and repeatable thermal response. When this mean U-value is converted by accounting for the 20 mm total plaster thickness on both sides, the effective thermal conductivity of the modified plaster is calculated as 0.04856 W/mK,

reaffirming the consistency of the material's insulating capability across consecutive days. As shown in Figure 5, the second-day measurements are presented in the same format. Additionally, the figure includes a direct comparison of U-values between the two test days, illustrating the consistency in thermal performance.

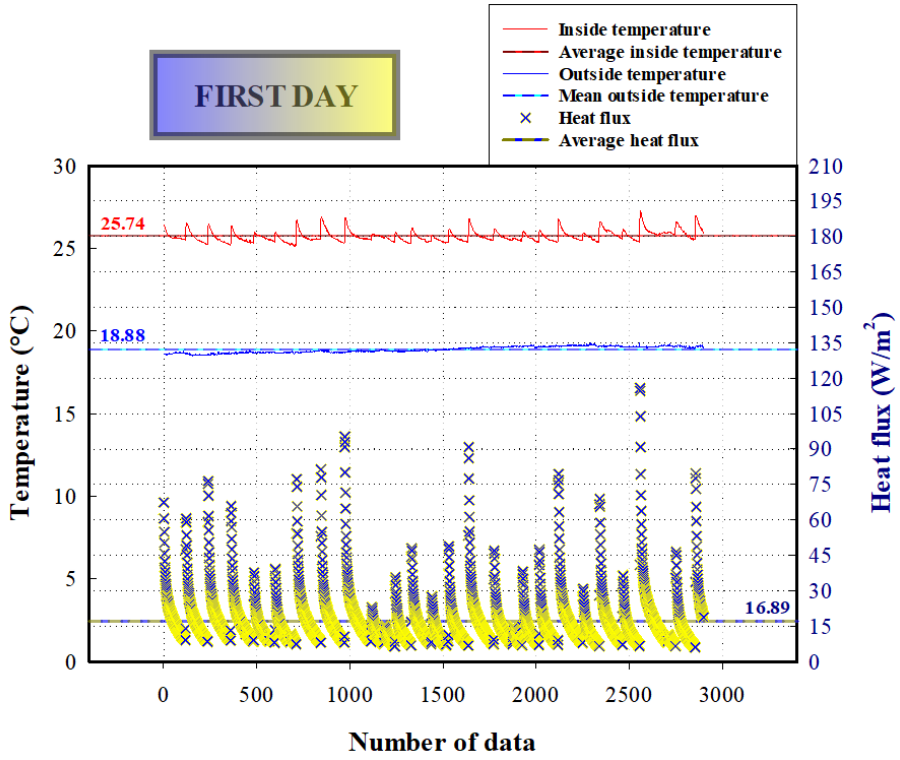

Figure 4. Thermal data on Day 1 for 2% hazelnut shell plaster.

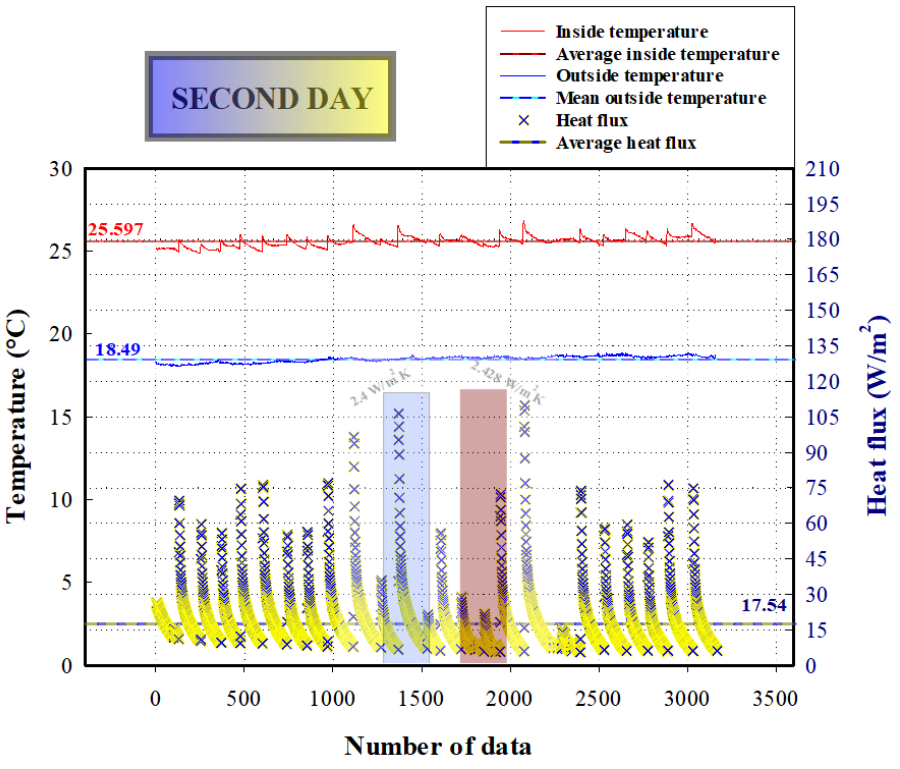

Figure 5. Thermal data and U-value comparison for 2% plaster on Day 2.

Thermal evaluation of plaster with 4% hazelnut shell, ground finely and applied as a 10 mm layer on the briquette, is carried out on the third day under identical laboratory conditions. The internal air temperature ranges between a minimum of 23.90 °C and a maximum of 27.15 °C, resulting in an average interior temperature of 25.55 °C. Concurrently, the exterior environment is maintained between 17.83 °C and 19.03 °C, with a mean outdoor temperature of 18.43 °C. The heat flux sensor records values from 3.02 W/m^2 up to 99.86 W/m^2, with an average flux of 15.45 W/m^2 across the effective measurement area. Based on these inputs, the U-value on the first test day fluctuates between 0.44 W/m^{2}K and 13.19 W/m^{2}K, yielding a daily average of 2.16 W/m^{2}K. By incorporating the total plaster thickness of 20 mm into this evaluation, the effective thermal conductivity of the modified layer is derived as 0.0432 W/mK, which demonstrates a noticeable improvement in insulation performance compared to the 2% mixture. Figure 6 shows the internal and external temperature trends, as well as the heat flux measurements, for the third test day of the 4% hazelnut shell-modified plaster sample. Both real-time values and daily averages are included. On the fourth day of testing, the internal temperature shows a slightly narrower range, from 24.74 °C to 27.08 °C, with a marginally higher mean of 25.80 °C. The outdoor temperature stabilises between 18.26 °C and 19.08 °C, averaging 18.75 °C. The heat flux profile ranges from 3.49 W/m^2 to 101.10 W/m^2, producing a mean value of 15.21 W/m^2. The corresponding U-value data vary from 0.49 W/m^{2}K to 13.60 W/m^{2}K, with an average U-value of 2.12 W/m^{2}K. When this mean U-value is translated into thermal conductivity by considering the 20 mm total plaster thickness, the effective k-value is determined as 0.0424 W/mK, further confirming the reproducibility and stability of the insulating behaviour observed on the previous day. Figure 7 presents the data recorded on the fourth test day. Additionally, a direct comparison of U-values between both test days is included to illustrate the consistency in thermal performance. Comparative analysis between the two test days reveals high consistency in thermal response. The variation in the average U-value is minimal, only 1.7% between the two trials, confirming the repeatability of the measurements and validating the reliability of the coheating test setup.

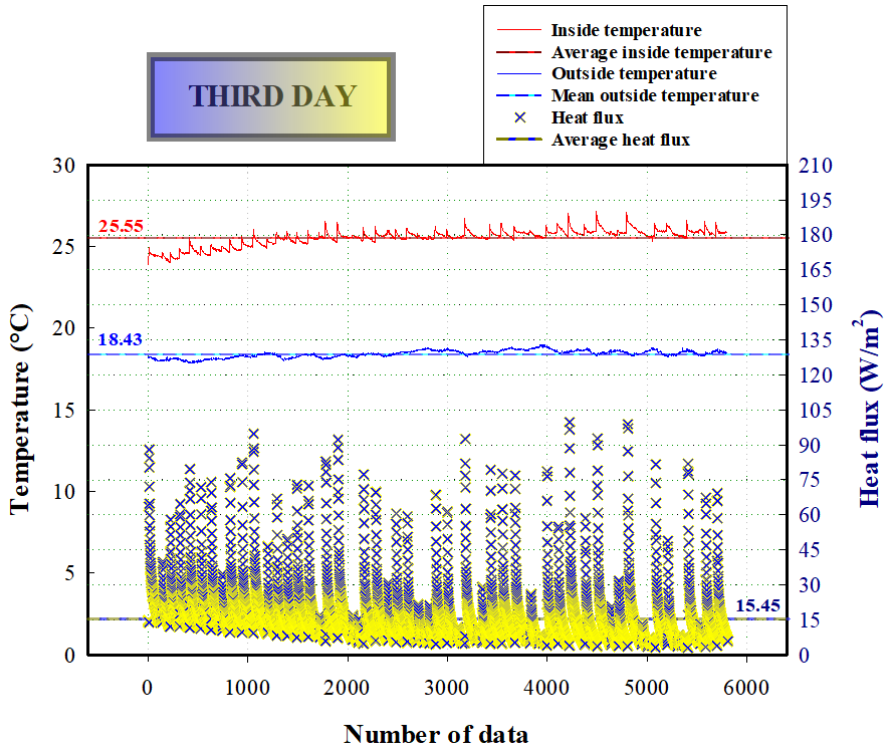

Figure 6. Thermal data on Day 3 for 4% hazelnut shell plaster.

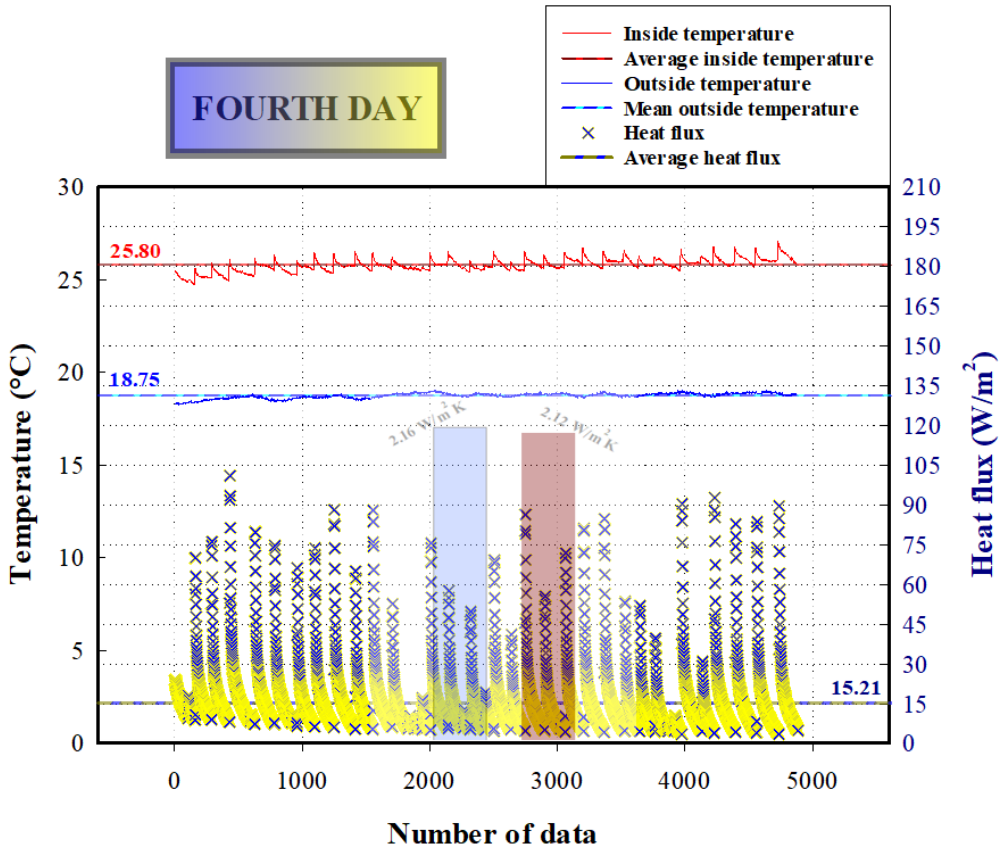

Figure 7. Thermal data and U-value comparison for 4% plaster on Day 4.

On the fifth day, the thermal performance of a 10 mm surface coating composed of plaster containing 6% finely milled hazelnut shells is evaluated. The internal temperature fluctuates between 24.87 °C and 27.19 °C, resulting in a daily average of 25.33 °C. The external environment remains steady, with recorded temperatures ranging from 18.51 °C to 18.96 °C, averaging 18.68 °C. Heat flux values observed span from 4.92 W/m^2 to 121.98 W/m^2, with a mean of 13.91 W/m^2. Based on these inputs, the U-value varies between 0.78 W/m^{2}K and 16.23 W/m^{2}K, yielding a mean U-value of 2.04 W/m^{2}K for the day. When translated into an equivalent conductivity using the cumulative plaster thickness of 20 mm, the resulting k-value is 0.0408 W/mK. This outcome indicates a further reduction compared to the 2% and 4% mixtures, emphasising the progressive improvement in insulation efficiency with increased hazelnut shell content. Figure 8 presents the thermal data obtained on the first test day of the 6% hazelnut shell-modified plaster sample, including internal and external temperatures, as well as heat flux values. Both real-time readings and daily averages are provided. On the sixth day, the test continues to be assessed under consistent experimental conditions. The internal temperature ranges from a minimum of 24.98 °C to a maximum of 27.86 °C, with a daily average of 25.73 °C. External environmental conditions remain stable, with outdoor temperatures fluctuating between 18.38 °C and 19.12 °C, with a mean value of 18.81 °C. Heat flux measurements recorded during the test span from 4.58 W/m^2 to 130.57 W/m^2, resulting in a mean daily heat flux of 14.76 W/m^2. From these thermal gradients and fluxes, the U-value for the plaster sample on day six is calculated to range between 0.69 W/m^{2}K and 16.70 W/m^{2}K, yielding an average U-value of 2.06 W/m^{2}K. When recalculated in terms of thermal conductivity by multiplying by the 20 mm plaster thickness, the obtained value is 0.0412 W/mK, which demonstrates that the insulating capacity of the 6% mixture remains consistently effective under prolonged testing. Figure 9 shows the second-day measurements for the same sample. It also includes a comparison of U-values from both test days, highlighting

the consistency and repeatability of thermal performance. A comparative evaluation between the fifth and sixth days indicates a high degree of measurement consistency. The average U-value on the fifth day was recorded as 2.04 W/m^{2}K, while the sixth day yielded a slightly higher average of 2.06 W/m^{2}K. This corresponds to a marginal increase of approximately 0.98%, underscoring the reliability and reproducibility of the thermal behaviour.

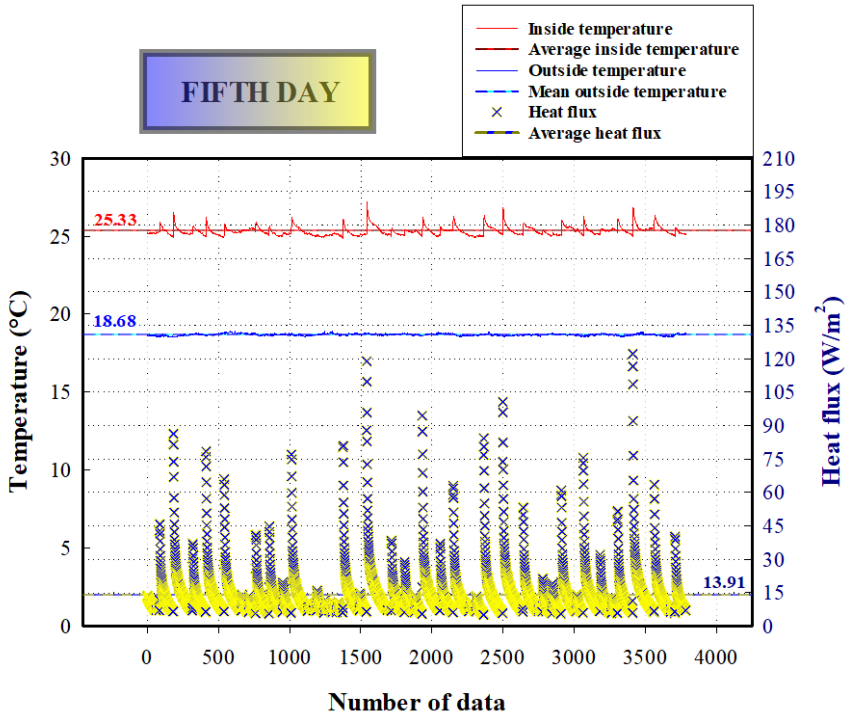

Figure 8. Thermal data on Day 5 for 6% hazelnut shell plaster.

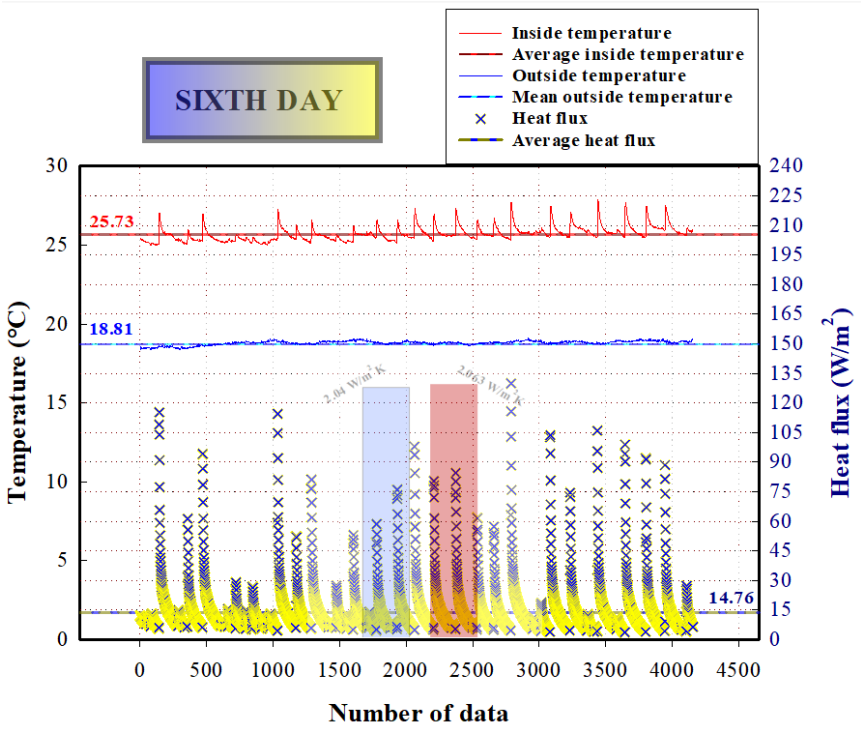

Figure 9. Thermal data and U-value comparison for 6% plaster on Day 6.

The findings of this study clearly indicate a substantial improvement in thermal insulation performance through the incorporation of finely ground hazelnut shells into

plaster formulations. Compared to the plain briquette sample, which exhibits a high U-value of 5.5 W/m^{2}K, all modified specimens demonstrate a dramatic reduction in heat transfer. The 2% hazelnut shell sample reduces the U-value to 2.40 W/m^{2}K, corresponding to a 56.4% improvement. The 4% sample performs even better, achieving an average U-value of 2.14 W/m^{2}K, a 61.1% mitigation, whilst the 6% formulation delivers the best result, with 2.04 W/m^{2}K, representing a 62.9% enhancement over the unmodified briquette. In addition to their performance against the control sample, a comparison among the hazelnut shell-modified specimens themselves provides further insight. As the substitution ratio increases from 2% to 6%, a clear downward trend in U-values is observed, signifying incremental improvements in thermal resistance. Specifically, the 6% sample achieves a 15% lower U-value than the 2% variant and 4.7% better than the 4% sample. These trends suggest a dose-dependent relationship between hazelnut shell content and insulating performance, likely attributed to increased porosity and reduced thermal conductivity within the plaster matrix as organic filler content rises.

The improvement in thermal resistance observed in hazelnut shell-modified plasters can be explained through several underlying mechanisms. The fragmented and porous morphology of the shells increases internal voids and introduces tortuous conduction paths, which slow down heat transfer across the plaster matrix. These pores and irregularities entrap air, a naturally low-conductivity medium, thereby further reducing thermal conductivity. In addition, the partial substitution of dense cementitious material with lightweight organic particles decreases the overall bulk density of the plaster, lowering its effective thermal conductance. The relatively high lignin content of hazelnut shells also provides inherent thermal stability, while their cellulose–hemicellulose fraction contributes to gradual heat absorption and release, enhancing the thermal buffering capacity. Taken together, these features clarify why the plaster formulations with higher shell content consistently deliver lower U-values, confirming that porosity, trapped air, reduced density, and distinctive lignocellulosic chemistry collectively drive the improved thermal insulation performance.

When benchmarked against earlier studies, the superiority of the current results becomes even more evident. A previous investigation by the authors achieved a minimum U-value of 2.86 W/m^{2}K through variation in plaster thickness [20], while another study involving bamboo-based substitution reported a best value of 2.77 W/m^{2}K [21]. Even the least effective hazelnut-modified sample in this work (2%) surpasses both prior benchmarks, demonstrating the significant potential of hazelnut shells as a sustainable and high-performance insulating additive. A fair benchmark with conventional solutions pairs U-values with thickness. Independent in situ measurements on sandwiched wall panels show that a section with a 50 mm XPS core between 75 mm + 75 mm concrete layers delivers an average U-value around 0.84 W/m^{2}K, whereas a companion panel with a 50 mm EPS-bead foam–mortar core of the same concrete layers reports about 2.53 W/m^{2}K [69]. In board-type products derived from conventional insulation, EPS waste + mineral-wool fibre gypsum boards used at nearly 25 mm thickness reduce density by approximately 20.3% and thermal conductivity by practically 30.4% relative to reference gypsum, confirming the performance space attainable with conventional-origin constituents at modest board thickness [70]. Against that backdrop, the present study pursues a different retrofit logic: instead of installing multi-centimetre boards that can encroach on usable floor area and complicate interior detailing, it integrates a thin render by applying 10 mm bio-based plaster directly onto a high-U briquette substrate. From a baseline around 5.5 W/m^{2}K, the daily average U-values fall to 2.40, 2.12, and 2.04 W/m^{2}K for the 2%, 4%, and 6% mixes, i.e., $\approx$ 56–63% reduction with minimal thickness. This thin-layer strategy therefore compares on multiple axes: (i) thickness-normalised impact, a 10 mm addition

yields about 3.1–3.5 W/m^{2}K absolute drop (virtually 0.31–0.35 per mm); (ii) space efficiency, no meaningful loss of interior volume or rework at reveals/services; (iii) constructability, render-based application over existing masonry rather than adding standalone boards; and (iv) resource valorisation, agro-waste utilisation with measurable thermal gains. In short, whilst thick EPS/XPS/mineral–wool boards can reach lower absolute U-values due to their high thickness, the thin-coating, high-baseline context here delivers a compelling relative performance per added millimetre without the aesthetic and area penalties of bulky layers. An additional noteworthy observation is the thermal inertia exhibited by the 6% hazelnut shell sample. During testing, this specimen displays a delayed internal temperature drop, indicating slower heat loss compared to others. This effect can be linked to the increased thermal mass and buffering capacity introduced by the higher organic content. Such behaviour is advantageous in real-world applications, as it reduces the demand on active heating systems and contributes to energy savings by prolonging indoor comfort conditions. Overall, the results not only validate the efficiency and repeatability of hazelnut shell-based plasters but also highlight their scalable potential as an eco-friendly insulation solution superior to several conventional alternatives.

Strengths, Limitations, Opportunities, and Threats (SWOT Analysis)

This study demonstrates several important strengths. The innovative use of finely ground hazelnut shells in plaster formulations achieves remarkable U-value reductions of 56–63% with only a 10 mm coating. The approach is cost-effective, scalable, and space-efficient, avoiding the drawbacks of bulky insulation boards while maintaining high repeatability, with day-to-day variation remaining below 2%. Furthermore, the method valorises an abundant agricultural waste stream, aligning with circular economy principles, and outperforms earlier bio-based additives such as bamboo or thickness-only plaster strategies.

At the same time, this study has some weaknesses that must be acknowledged. The results are derived exclusively from laboratory-scale coheating tests and therefore do not fully represent real building conditions. Durability aspects such as resistance to moisture, freeze–thaw behaviour, fire performance, and mechanical stability are not evaluated within the present scope. The investigation is limited to a single masonry briquette type with a fixed plaster thickness, which restricts the generalisability of the findings across different wall systems and climates. In addition, aspects such as acoustic behaviour, economic feasibility, and life-cycle assessment remain unexplored.

Beyond its current scope, this study also offers several opportunities. The findings open a pathway for large-scale applications in low-cost housing and rural retrofitting programmes. Future work may expand the approach to different wall systems, climates, and construction types, as well as integrate hazelnut shell-modified plaster with other eco-friendly materials, such as natural fibres or phase change materials. This line of research aligns strongly with policy agendas on sustainable construction and decarbonisation targets, particularly given the growing global demand for circular-economy building materials.

Nevertheless, there are potential threats that could challenge widespread adoption. Long-term durability under real environmental conditions remains uncertain, and the technology must compete with well-established commercial insulation products, such as XPS and mineral wool. Regulatory approval processes and the need for standardisation may also delay its uptake. Furthermore, variability in the supply of agricultural waste due to regional and seasonal factors could constrain scalability, while practical concerns regarding fire resistance and structural performance will need to be addressed before broad market acceptance is achieved. These strengths, limitations, opportunities, and threats are visually summarised in Figure 10, which presents a SWOT analysis of this study.

Figure 10. SWOT analysis of the present study, highlighting strengths, weaknesses, opportunities, and threats associated with hazelnut shell-modified insulation plasters.

4. Conclusions

This research introduces a cost-effective and environmentally sustainable facade retrofitting strategy by incorporating finely milled hazelnut shells into thermal insulation plaster applied symmetrically to both sides of masonry briquettes. This approach aligns with circular economy principles and addresses the dual objectives of energy efficiency and material valorisation in the building sector. The experimental results obtained via coheating tests show a clear, dose-dependent improvement in thermal resistance. Compared to the uncoated control sample (5.5 W/m^{2}K), U-values are reduced to 2.40 W/m^{2}K with 2% shell content (56.4% improvement), 2.14 W/m^{2}K with 4% (61.1%), and 2.04 W/m^{2}K with 6% (62.9%). The 6% sample not only delivers the lowest U-value but also demonstrates improved thermal inertia, reducing heat loss rate and maintaining interior thermal comfort for longer durations. By translating U-values into equivalent thermal conductivity, the effective k-values of the modified plaster layers are found to be 0.04856 W/mK (2%), 0.0432 W/mK (4%), and 0.0408 W/mK (6%), all of which are markedly lower than conventional plaster (~0.72–0.80 W/mK) and competitive with other bio-based insulation composites. These results confirm that hazelnut shell-modified plasters offer an exceptionally low-conductivity pathway for enhancing thermal performance without increasing plaster thickness, highlighting their strong potential in sustainable retrofitting. In addition to strong repeatability and high reliability of the test outcomes, this study confirms that hazelnut shell-modified plasters outperform previous bio-based solutions, such as bamboo-reinforced composites or plaster thickness increases. These findings suggest that finely milled hazelnut shells offer a superior insulation pathway due to their low thermal conductivity, porous structure, and fibrous morphology.

Key highlights and implications are given below:

- All modified plasters achieve over 56% improvement in thermal resistance, with the 6% shell content reducing U-value by 62.9%, outperforming all prior benchmarks.

- Effective thermal conductivity values of 0.0408–0.048 W/mK confirm the strong insulating behaviour of the composites and their competitiveness with other bio-based insulators.
- Increasing shell content consistently enhances thermal performance, with the 4% formulation showing 61.1% improvement, ideal for balanced cost–performance applications.
- All three formulations exceed U-value reductions previously reported for bamboo composites or increased plaster thickness.
- The 6% sample delays heat transfer more effectively, contributing to passive thermal buffering and reduced heating demand.
- The approach offers scalable, low-cost retrofitting for low-income housing, rural infrastructure, and public refurbishment schemes, particularly in regions rich in agricultural residues.
- The findings support building decarbonisation strategies under national and global climate targets and provide a model for bio-based construction standards.
- Further research will focus on evaluating the durability of hazelnut shell-modified plasters under moisture exposure, their reparability and recycling potential, and their applicability across diverse climate zones. Additional assessments on fire resistance, acoustic performance, and mechanical stability are also planned, ensuring a more comprehensive characterisation of these bio-based plaster composites in forthcoming studies.

Author Contributions: Conceptualization, P.M.C. and E.C.; methodology, P.M.C., E.C. and E.A.; software, E.A.; validation, P.M.C. and E.C.; formal analysis, E.A.; data curation, E.A.; writing—original draft preparation, E.A. and P.M.C.; writing—review and editing, P.M.C., E.C. and E.A.; project administration, P.M.C. All authors have read and agreed to the published version of the manuscript.

Funding: This research was funded by the Scientific Research Projects Coordination Unit under the standart research project scheme (Project ID: 1984, Project Code: FBA-2025-1984). The project supported the acquisition of experimental measurement equipment.

Data Availability Statement: All data covered in this paper are available from the corresponding author upon request.

Conflicts of Interest: The authors declare no conflicts of interest.

References

1. Bortone, I.; Sakar, H.; Soares, A. Gaps in regulation and policies on the application of green technologies at household level in the United Kingdom. *Sustainability* **2022**, *14*, 4030. [CrossRef]
2. Bayraktar, M.; Binatlı, B.; Üzümoğlu, T. WRI Türkiye Leads Development of Turkey's First Building Decar-bonization Roadmap. Republic of Türkiye Ministry of Environment, Urbanization and Climate Change: Ankara, Turkey, 2024; pp. 1–68. Available online: https://www.wri.org/update/wri-turkiye-first-building-decarbonization-roadmap (accessed on 2 July 2025).
3. Alvur, E.; Anaç, M.; Cuce, P.M.; Cuce, E. The Potential and Challenges of BIM in Enhancing Energy Efficiency in Existing Buildings: A Comprehensive Review. *Sustain. Clean Build.* **2024**, *1*, 42–65.
4. Zhen, X.; Li, S.; Peng, J.; Zhao, Z.; Zhang, X.; Tan, C.; Jiao, R.; Wu, W. Analysis of Building Envelope for Energy Consumption and Indoor Comfort in a Near-Zero-Energy Building in Northwest China. *Results Eng.* **2025**, *25*, 104243. [CrossRef]
5. Wang, Y.; Sun, G.; Wu, Y.; Rosenberg, M.W. Urban 3D building morphology and energy consumption: Empirical evidence from 53 cities in China. *Sci. Rep.* **2024**, *14*, 12887. [CrossRef] [PubMed]
6. Chapa, J. Bringing embodied carbon upfront. *Built. Environ. Econ. Aust. New Zealand* **2019**, 38–41. Available online: https://search.informit.org/doi/abs/10.3316/informit.985354490427057 (accessed on 2 July 2025).
7. Burnett, N.; Edwards, T.; Watson, N. *The UK's Plans and Progress to Reach Net Zero by 2050*; House of Commons Library: London, UK, 2024.
8. Zhou, S.; Tong, Q.; Pan, X.; Cao, M.; Wang, H.; Gao, J.; Ou, X. Research on low-carbon energy transformation of China necessary to achieve the Paris agreement goals: A global perspective. *Energy Econ.* **2021**, *95*, 105137. [CrossRef]

9. United Nations. Sustainable Development Goals. Available online: https://sdgs.un.org/goals (accessed on 2 July 2025).
10. Onyenokporo, N.C.; Taki, A.; Montalvo, L.Z.; Oyinlola, M.A. Exploring the impact of rice husk ash masonry blocks on building energy performance. *Buildings* **2024**, *14*, 1290. [CrossRef]
11. Harish, V.S.K.V.; Kumar, A. A review on modeling and simulation of building energy systems. *Renew. Sustain. Energy Rev.* **2016**, *56*, 1272–1292. [CrossRef]
12. Efficiency IE. *Buildings*; International Energy Agency: Paris, France, 2018.
13. Fattahi, M.; Taban, E.; Soltani, P.; Berardi, U.; Khavanin, A.; Zaroushani, V. Waste corn husk fibers for sound absorption and thermal insulation applications: A step towards sustainable buildings. *J. Build. Eng.* **2023**, *77*, 107468. [CrossRef]
14. Yang, L.; Yang, J.; Liu, Y.; An, Y.; Chen, J. Hot box method to investigate U-values for straw bale walls with various structures. *Energy Build.* **2021**, *234*, 110706. [CrossRef]
15. Shea, A.; Wall, K.; Walker, P. Evaluation of the thermal performance of an innovative prefabricated natural plant fibre building system. *Build. Serv. Eng. Res. Technol.* **2013**, *34*, 369–380. [CrossRef]
16. Seifhashemi, M.; Elkadi, H.A.; Fitton, R. The impact of baseline wall U-value on energy performance of solid wall insulation. In Proceedings of the 5th Building Simulation and Optimization Virtual Conference, Loughborough, UK, 21–22 September 2020.
17. Platt, S.L.; Walker, P.; Maskell, D.; Shea, A.; Bacoup, F.; Mahieu, A.; Zmamou, H.; Gattin, R. Sustainable bio & waste resources for thermal insulation of buildings. *Constr. Build. Mater.* **2023**, *366*, 130030. [CrossRef]
18. Dams, B.; Cascione, V.; Shea, A.; Maskell, D.; Allen, S.; Walker, P.; Emmitt, S. An investigation into the thermal and hygric performance of bio-based wall systems. *J. Build. Eng.* **2025**, *101*, 111727. [CrossRef]
19. Elkhayat, Y.O.; Elmozy, S.A.; El-Darwish, I.I. Selecting the Optimal Thermal Insulation Material for a Residential Building Envelope in Cairo in Consideration of The Thermal Comfort and Energy Consumption. *J. Sustain. Archit. Civ. Eng.* **2023**, *33*, 122–132. [CrossRef]
20. Cuce, E.; Cuce, P.M.; Alvur, E.; Yilmaz, Y.N.; Saboor, S.; Ustabas, I.; Linul, E.; Asif, M. Experimental performance assessment of a novel insulation plaster as an energy-efficient retrofit solution for external walls: A key building material towards low/zero carbon buildings. *Case Stud. Therm. Eng.* **2023**, *49*, 103350. [CrossRef]
21. Cuce, P.M.; Alvur, E.; Cuce, E.; Alshahrani, S.; Prakash, C.; Tan, H.; Ustabas, I. Unlocking energy efficiency: Experimental investigation of bamboo fibre reinforced briquettes as sustainable solution with enhanced thermal resistance. *Case Stud. Therm. Eng.* **2024**, *60*, 104680. [CrossRef]
22. Kamble, G.S.; Upadhye, A.V.; Bhise, R.R.; Yammi, N.V.; Kumbhar, D.P.; Panwal, N.G. Study of Heat Transfer Through Porous-Brick Wall with Green Insulation Developed for Sustainable Infrastructure. *Mater. Circ. Econ.* **2025**, *7*, 9. [CrossRef]
23. Bendaikha, W.; Allouche, F.N.; Abdeladim, K.; Bouabidi, A.; Cuce, E. The investigation of thermal insulation property of the pine needle waste. *J. Therm. Anal. Calorim.* **2025**, *150*, 5911–5919. [CrossRef]
24. Messahel, B.; Onyenokporo, N.; Beizaee, A.; Oyinlola, M. Thermal characterisation of composite walls made from waste materials. In Proceedings of the 16th International Conference on Heat Transfer, Fluid Mechanics and Thermodynamics (HEFAT, HEFAT2022-ATE), Online, 8–10 August 2022.
25. Rashid, K.; Haq, E.U.; Kamran, M.S.; Munir, N.; Shahid, A.; Hanif, I. Experimental and finite element analysis on thermal conductivity of burnt clay bricks reinforced with fibers. *Constr. Build. Mater.* **2019**, *221*, 190–199. [CrossRef]
26. Charai, M.; Sghiouri, H.; Mezrhab, A.; Karkri, M. Thermal insulation potential of non-industrial hemp (Moroccan *Cannabis sativa* L.) fibers for green plaster-based building materials. *J. Clean. Prod.* **2021**, *292*, 126064. [CrossRef]
27. Nasreddine, H.; Salem, T.; Omikrine-Metalssi, O.; Fen-Chong, T. Potential use of human hair fibers for reinforcement and thermal insulation in construction. *J. Mater. Cycles Waste Manag.* **2024**, *26*, 970–985. [CrossRef]
28. Ali, M.; Al-Suhaibani, Z.; Almuzaiqer, R.; Al-Salem, K.; Nuhait, A.; Algubllan, F.; Al-Howaish, M.; Aloraini, A.; Alqahtani, I. Sunflower and watermelon seeds and their hybrids with pineapple leaf fibers as new novel thermal insulation and sound-absorbing materials. *Polymers* **2023**, *15*, 4422. [CrossRef] [PubMed]
29. Ba, L.; Kane, C.S.E.; Darcherif, I.; Pliya, P.; Ngo, T.T.; Niang, I.; Haidara, F. Experimental and numerical investigation of energy performance of building using biobased materials for sustainable construction. *Energy Effic.* **2023**, *16*, 78. [CrossRef]
30. Łapka, P.; Dietrich, F.; Furmański, P.; Sinka, M.; Sahmenko, G.; Bajare, D. Experimental and numerical estimation of thermal conductivity of bio-based building composite materials with an enhanced thermal capacity. *J. Energy Storage* **2024**, *97*, 112943. [CrossRef]
31. Blanco, J.M.; Frómeta, Y.G.; Madrid, M.; Cuadrado, J. Thermal performance assessment of walls made of three types of sustainable concrete blocks by means of fem and validated through an extensive measurement campaign. *Sustainability* **2021**, *13*, 386. [CrossRef]
32. Briga-Sá, A.; Gaibor, N.; Magalhaes, L.; Pinto, T.; Leitao, D. Thermal performance characterization of cement-based lightweight blocks incorporating textile waste. *Constr. Build. Mater.* **2022**, *321*, 126330. [CrossRef]
33. El-Lawindy, A.E.-R.; Abdelkader, H.H.; Abdullah, A.A.; Khalil, M.; Abobakr, S.M. The Role of Agriculture Waste in Achieving High Efficacy in Residential Sustainable Buildings in Egypt. *Int. J. Ind. Sustain. Dev.* **2024**, *5*, 83–94. [CrossRef]

34. Ahmed, S.; El Attar, M.E.; Zouli, N.; Abutaleb, A.; Maafa, I.M.; Ahmed, M.M.; Yousef, A.; Ragab, A. Improving the thermal performance and energy efficiency of buildings by incorporating biomass waste into clay bricks. *Materials* **2023**, *16*, 2893. [CrossRef]
35. Ahmed, M.M.; Ali, S.A.; Tarek, D.; Maafa, I.M.; Abutaleb, A.; Yousef, A.; Fahmy, M.K. Development of bio-based lightweight and thermally insulated bricks: Efficient energy performance, thermal comfort, and CO_2 emission of residential buildings in hot arid climates. *J. Build. Eng.* **2024**, *91*, 109667. [CrossRef]
36. Jiang, Z.; He, G.; Jiang, Y.; Zhao, H.; Duan, Y.; Yuan, G.; Fu, H. Synergistic preparation and properties of ceramic foams from wolframite tailings and high-borosilicate waste glass. *Constr. Build. Mater.* **2024**, *457*, 139367. [CrossRef]
37. Xu, Y.; Fan, Z.; Li, X.; Yang, S.; Wang, J.; Zheng, A.; Shu, R. Cooperative production of monophenolic chemicals and carbon adsorption materials from cascade pyrolysis of acid hydrolysis lignin. *Bioresour. Technol.* **2024**, *399*, 130557. [CrossRef]
38. Ozocak, M.; Sisman, C.B. Development of a new insulation material from hazelnut shells (hazelnut shell insulation board–HSIB). *J. Elem.* **2024**, *29*, 293–310.
39. Cuce, E.; Cuce, P.M.; Wood, C.; Gillott, M.; Riffat, S. Experimental investigation of internal aerogel insulation towards low/zero carbon buildings: A comprehensive thermal analysis for a UK building. *Sustain. Clean Build.* **2024**, *1*, 1–22.
40. Cuce, E.; Cuce, P.M. The impact of internal aerogel retrofitting on the thermal bridges of residential buildings: An experimental and statistical research. *Energy Build.* **2016**, *116*, 449–454. [CrossRef]
41. Arregi, B.; Garay-Martinez, R.; Astudillo, J.; García, M.; Ramos, J.C. Experimental and numerical thermal performance assessment of a multi-layer building envelope component made of biocomposite materials. *Energy Build.* **2020**, *214*, 109846. [CrossRef]
42. Cuce, P.M.; Cuce, E.; Alvur, E. Internal or external thermal superinsulation towards low/zero carbon buildings? A critical report. *Gazi Mühendis. Bilim. Derg.* **2024**, *9*, 435–442.
43. Cuce, E.; Cuce, P.M. Optimised performance of a thermally resistive PV glazing technology: An experimental validation. *Energy Rep.* **2019**, *5*, 1185–1195. [CrossRef]
44. Pourghorban, A.; Asoodeh, H. The impacts of advanced glazing units on annual performance of the Trombe wall systems in cold climates. *Sustain. Energy Technol. Assess.* **2022**, *51*, 101983. [CrossRef]
45. Simões, N.; Manaia, M.; Simões, I. Energy performance of solar and Trombe walls in Mediterranean climates. *Energy* **2021**, *234*, 121197. [CrossRef]
46. Cuce, E. Experimental and numerical investigation of a novel energy-efficient vacuum glazing technology for low-carbon buildings. *Indoor Built Environ.* **2017**, *26*, 44–59. [CrossRef]
47. Liu, X.; Yang, H.; Wang, C.; Shen, C.; Bo, R.; Hinkle, L.; Wang, J. Semi-experimental investigation on the energy performance of photovoltaic double skin façade with different façade materials. *Energy* **2024**, *295*, 131049. [CrossRef]
48. Peng, J.; Lu, L.; Yang, H.; Ma, T. Comparative study of the thermal and power performances of a semi-transparent photovoltaic façade under different ventilation modes. *Appl. Energy* **2015**, *138*, 572–583. [CrossRef]
49. Es-Sakali, N.; Kaitouni, S.I.; Ait Laasri, I.; Mghazli, M.O.; Cherkaoui, M.; Pfafferott, J. Static and dynamic glazing integration for enhanced building efficiency and indoor comfort with thermochromic and electrochromic windows. *Therm. Sci. Eng. Prog.* **2024**, *52*, 102681. [CrossRef]
50. Hong, X.; Shi, F.; Wang, S.; Yang, X.; Yang, Y. Multi-objective optimization of thermochromic glazing based on daylight and energy performance evaluation. *Build. Simul.* **2021**, *14*, 1685–1695. [CrossRef]
51. Butt, A.A.; de Vries, S.B.; Loonen, R.C.; Hensen, J.L.; Stuiver, A.; van den Ham, J.E.; Erich, B.S. Investigating the energy saving potential of thermochromic coatings on building envelopes. *Appl. Energy* **2021**, *291*, 116788. [CrossRef]
52. Zakaria, N.M.; Omar, M.A.; Mukhtar, A. Numerical study on the thermal insulation of smart windows embedded with low thermal conductivity materials to improve the energy efficiency of buildings. *CFD Lett.* **2023**, *15*, 41–52. [CrossRef]
53. Abdelrady, A.; Abdelhafez, M.H.H.; Ragab, A. Use of insulation based on nanomaterials to improve energy efficiency of residential buildings in a hot desert climate. *Sustainability* **2021**, *13*, 5266. [CrossRef]
54. Li, X.; Wu, Y. A review of complex window-glazing systems for building energy saving and daylight comfort: Glazing technologies and their building performance prediction. *J. Build. Phys.* **2025**, *48*, 496–540. [CrossRef]
55. Cuce, E.; Cuce, P.M. Solar pond window technology for energy-efficient retrofitting of buildings: An experimental and numerical investigation. *Arab. J. Sci. Eng.* **2017**, *42*, 1909–1916. [CrossRef]
56. Tan, Y.; Peng, J.; Luo, Y.; Luo, Z.; Curcija, C.; Fang, Y. Numerical heat transfer modeling and climate adaptation analysis of vacuum-photovoltaic glazing. *Appl. Energy* **2022**, *312*, 118747. [CrossRef]
57. Radwan, A.; Katsura, T.; Memon, S.; Serageldin, A.A.; Nakamura, M.; Nagano, K. Thermal and electrical performances of semi-transparent photovoltaic glazing integrated with translucent vacuum insulation panel and vacuum glazing. *Energy Convers. Manag.* **2020**, *215*, 112920. [CrossRef]
58. Ghosh, A.; Sundaram, S.; Mallick, T.K. Investigation of thermal and electrical performances of a combined semi-transparent PV-vacuum glazing. *Appl. Energy* **2018**, *228*, 1591–1600. [CrossRef]

59. Lami, M.; Al-Naemi, F.; Jabbar, H.; Alrashidi, H.; Issa, W. Thermal Loss Reduction Using a Ventilated Double-Glazed Window for Commercial Buildings in Average-Climate Environments. In Proceedings of the International Conference on Sustainable Energy Engineering and Application (ICSEEA), Singapore, 3–5 February 2021.
60. Naqash, M.T. Analyzing glass configurations for energy efficiency in building envelopes: A comparative study. *J. Appl. Sci. Eng.* **2025**, *28*, 319–333.
61. Awale, A.; Uprety, S. Impact of Window-Wall Ratio on Heating and Cooling Energy Consumption: A Case of Office Building in Kathmandu. In Proceedings of the 10th IOE Graduate Conference, Dharan, Nepal, 30 September–2 October 2021; Volume 10, pp. 898–904.
62. Vijayan, D.S.; Sivasuriyan, A.; Patchamuthu, P.; Jayaseelan, R. Thermal performance of energy-efficient buildings for sustainable development. *Environ. Sci. Pollut. Res.* **2022**, *29*, 51130–51142. [CrossRef] [PubMed]
63. Sia, B.K.H.; Ariff, M.A.M. Enhancement of energy efficiency and sustainability through green building index platinum certification in Malaysian building design. *Majlesi J. Electr. Eng.* **2025**, *19*, 1–17.
64. FAOSTAT. FAO Hazelnut Production Statistics of Countries in 2023. Food and Agriculture Organization Statistics 2024. Available online: https://www.fao.org/faostat/en/#data/QCL (accessed on 7 July 2025).
65. Fuso, A.; Risso, D.; Rosso, G.; Rosso, F.; Manini, F.; Manera, I.; Caligiani, A. Potential valorization of hazelnut shells through extraction, purification and structural characterization of prebiotic compounds: A critical review. *Foods* **2021**, *10*, 1197. [CrossRef]
66. Deconinck, A.H.; Roels, S. Reliable Thermal Resistance Estimation of Building Components from On-Site Measurements. Ph.D. Thesis, KU Leuven, Leuven, Belgium, 2017.
67. Krstić, H.; Domazetović, M. Co-heating test as a tool for reduction of energy performance gap in buildings. *Int. J. Energy Prod. Manag.* **2020**, *5*, 328–341. [CrossRef]
68. Coleman, H.W.; Steele, W.G. *Experimentation, Validation, and Uncertainty Analysis for Engineers*; John Wiley & Sons: Hoboken, NJ, USA, 2009; p. 3.
69. Alhems, L.M.; Ahmad, A.; Ibrahim, M.; Ali, M.R.; Al-Shugaa, M.A. Comparative Thermal Evaluation of Two Systems of Wall Panels Exposed to Hot and Arid Arabian Environmental Weather Conditions. *Int. J. Concr. Struct. Mater.* **2024**, *18*, 35. [CrossRef]
70. Zaragoza-Benzal, A.; Ferrández, D.; Santos, P.; Atanes-Sánchez, E. Upcycling EPS waste and mineral wool to produce new lightweight gypsum composites with improved thermal performance. *Constr. Build. Mater.* **2024**, *449*, 138464. [CrossRef]